phys. stat. sol. (a) **199**, No. 2, 207–213 (2003) / **DOI** 10.1002/pssa.200306656

Defects in silicon heat-treated under uniform stress and irradiated with fast neutrons

I. V. Antonova[1], **C. A. Londos**[*, 2], **J. Bak-Misiuk**[3], **A. K. Gutakovskii**[1], **M. S. Potsidi**[2], and **A. Misiuk**[4]

[1] Institute of Semiconductor Physics, Pr. Lavrentyeva 13, 630090 Novosibirsk, Russia
[2] Solid State Section, Physics Department, University of Athens, Panepistimiopolis, Zografos, 157 84 Athens, Greece
[3] Institute of Physics, Polish Academy of Sciences, Al. Lotnikow 46, 02-668 Warsaw, Poland
[4] Institute of Electron Technology, Al. Lotnikow 32/46, 02-668 Warszawa, Poland

Received 24 March 2003, revised 1 July 2003, accepted 8 July 2003
Published online 17 September 2003

PACS 61.72.–y, 61.80.Hg, 61.82.Fk, 78.20.–e

Silicon samples of initial oxygen concentration $[O_i]_o \sim 8.3 \times 10^{17}$ cm^{-3} were subjected to various high temperature–high pressure (HT–HP) treatments in the temperature range 900–1050 °C. Afterwards, the samples were irradiated by fast neutrons and then isothermally annealed at 400 °C. Infrared spectroscopy, X-ray diffraction, transmission electron microscopy (TEM), optical spectroscopy and selective etching measurements were performed. Besides the precipitates and the dislocation loops that usually form, small defect clusters were also detected in the samples. The presence of these clusters is revealed due to their decoration with radiation induced point defects, and attributed to the HP treatment.

1 Introduction

Application of enhanced hydrostatic pressure, in argon atmosphere, during heat treatment of Czochralski grown silicon samples (Cz–Si), results in generation of defects, in stress-induced oxygen precipitation, in pressure-stimulated creation of TDs, as well as in some other HP-related phenomena [1–3]. One of the main HP-related effects is the enhanced formation of the "old" and "new" TDs [4–6]. Two reasons are usually discussed [3–6] as explanation of the enhanced TDs formation: (i) the enhanced oxygen diffusion and (ii) the HP-stimulated introduction of TD nuclei or nucleation sites. Nevertheless, the picture is not yet clear. Concerning oxygen diffusion for instance, there are also reports [7], which argue that at high temperatures (≥ 900 °C) the oxygen diffusion coefficient decreases under HP conditions, in comparison to that under atmospheric pressure conditions. Thus, more light has to be shed, in order to elaborate the role of pressure in these phenomena. In addition, the issue of the TDs nuclei is still open and more importantly their exact nature has not been determined so far. The application of external pressure is expected to improve our understanding of the formation mechanism of TDs.

In this article, we report on the presence of unknown nature small defects created in the HT–HP treated Cz–Si crystals subjected to neutron irradiation and subsequent annealing. The defects form as a result of the HP treatment but their presence is revealed due to their decoration with radiation-induced point defects. In the present work we study these small defects and suggest the connection of their presence with HT–HP-related effects.

[*] Corresponding author: e-mail: hlontos@cc.uoa.gr, Phone: +003 210 7276726, Fax: +003 210 7276726

Table 1 Values of the initial oxygen interstitial concentration $[O_i]_o$, the oxygen concentration after treatments at different HT–HP conditions, after neutron irradiation and after annealing at 220 °C, for 150 h and at 400 °C, for 4 h.

Sample	Initial oxygen concentration $[O_i] \times 10^{17}$ (cm^{-3})	HT–HP conditions T (°C), P (Kbar), t (h)	Oxygen concentration after HT–HP treatment $[O_i] \times 10^{17}$ (cm^{-3})	Oxygen concentration after neutron irradiation $[O_i] \times 10^{17}$ (cm^{-3})	Oxygen concentration after the two anneals $[O_i] \times 10^{17}$ (cm^{-3})
T0	8.33	untreated	8.33	8.16	8.01
T1-1	8.33	900, 3, 3	7.94	8.24	7.86
T1-2	8.33	900, 12, 5	6.28	6.40	6.18
T1-3	8.33	900, 12, 10	4.16	4.25	4.20
T2	8.33	957, 12, 10	3.06	3.26	3.17
T3	8.33	1027, 12, 5	5.33	5.24	5.10

2 Experimental details

Six samples cut from a 2 mm thick, 001 oriented wafer, were used. Their initial oxygen concentration was $[O_i]_o \sim 8.3 \times 10^{17}$ cm^{-3}. The samples were subjected to various combinations of HT–HP treatments as shown in Table 1 and then irradiated by fast neutrons at a fluence of $\sim 1 \times 10^{17}$ cm^{-2}, at a temperature T around 50 °C. Then, the samples were subjected to isothermal anneals at 220 °C for 150 hours, at atmospheric pressure, aiming at the out-annealing of the large clusters of defects and disordered regions, present [8] in neutron-irradiated material. Finally, the samples were subjected to a heat treatment at 400 °C, for 4 h, at atmospheric pressure. During the latter heat treatment the main radiation defects, that is, divacancies and VO complexes as well as the vacancy-type and the interstitial-type defects are expected [9–12] to be destroyed and new, more complex defect structures to form. The purpose of the latter anneal was to decorate the HT–HP related defects with defects introduced by neutron irradiation and the subsequent anneals. The established values of $[O_i]$ after these processes are also cited in Table 1.

We study the HT–HP related defects by employing a number of experimental techniques involving X-ray diffraction, optical microscopy on samples subjected to selective etching and transmission electron microscopy (TEM) measurements. Infrared spectra were taken at room temperature by a dispersive kind spectrometer. The concentration of interstitial oxygen $[O_i]$ was monitored by measuring the well known absorption band at 1107 cm^{-1} using a calibration coefficient equal to 2.45×10^{17} cm^{-2}. X-ray investigations were performed using a high-resolution diffractometer in double configuration. Rocking curves and reciprocal space maps were recorded for all samples. A high-resolution experimental set-up was realised by employing a four-crystal Ge (220) Bartels-type monochromator in the primary beam and a channel-cut double-reflection Ge (220) analyser in the diffracted beam. The selective etching was performed in

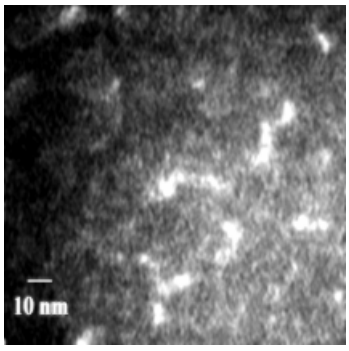

Fig. 1 Plan-view TEM image for the sample T0.

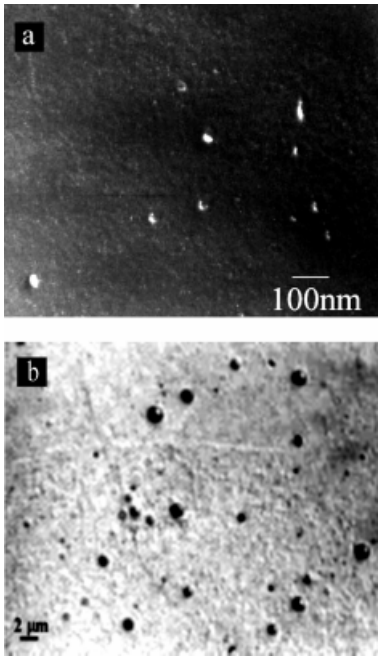

Fig. 2 a) Plan-view TEM image and b) surface image after selective etching for the sample T1-1 treated at 900 °C for 3 h at 3 kbar.

Sirtle solution (33% CrO_3: HF in proportion 1 : 2) for 5 min. Optical images of surface of the samples were obtained by means of micromanipulator MickroZoom II, Polaroid type Photomicrographics and PCI plate MiroVideo (Pinnacle System). TEM investigations were carried out with an electron microscope JEOL EM-4000 EX operated at 400 kV. The samples for TEM measurements were prepared in form of thin foils parallel to the (001) sample surface. The plane-view (100) foils were prepared using the jet chemical etching in solution 1 HF + 5 HNO_3 from the back side of the sample. The analysis of dislocation structure was carried out under the two-beam diffraction conditions from the {220} and {400} planes. The methods bright and dark field and weak beam were used.

3 Experimental results

The plan-view TEM image for the untreated sample T0 is presented in Fig. 1. Small stressed areas are observed in the TEM image of this sample. The reciprocal space map around the 004 reciprocal space point also shows stressed areas indicating the presence of defects in considerable concentration. Selective etching does not show the presence of defects. The observed stressed areas are most likely related to clusters of radiation defects introduced by neutron irradiation and subsequent annealing.

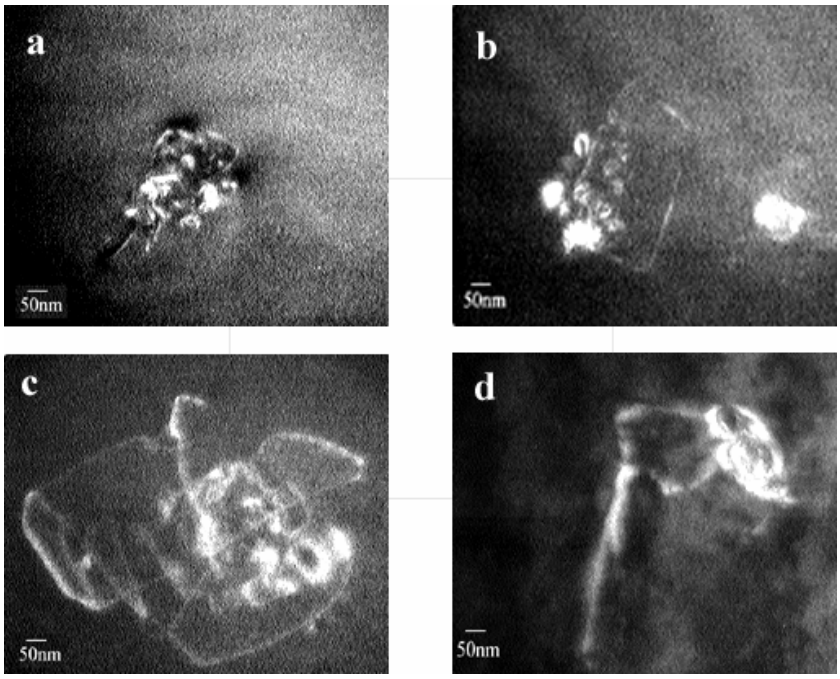

Fig. 3 Plan-view TEM images for the samples a)T1-2, b)T1-3, c) T2 and d) T3.

The sample T1-1 was treated at a relatively low pressure (3 kbar). Note, that treatments at such a pressure have almost similar effect with treatments at atmospheric pressure [3, 7]. TEM images show that small stressed areas are still present in this sample, while some relatively large defects, of 8×10^8 cm^{-2} density also appear (Fig. 2a). The surface image of this sample after selective etching also shows the appearance of hillocks, in concentration of 2×10^6 cm^{-2} (Fig. 2b). The relatively large defects observed by TEM and the hillocks observed by optical microscopy are most likely [9] oxygen precipitates (OPs), which begin to form in this sample.

The TEM images of the samples T1-2, T1-3, T2 and T3, treated at 12 kbars, show as expected [3–7, 13] the most pronounced pressure-related effect on the defect structure (Fig. 3). Relatively large oxygen precipitates with dislocation loops around them are seen. The density of these OPs estimated for the sample T1-2 is 2×10^8 cm^{-2}. An increase in the time of the treatment leads to an increase in the size of the defect agglomerates (OPs and the surrounding dislocation loops), as can be seen by comparing the TEM images of the samples T1-2 and T1-3. Furthermore, an increase in the temperature of the HT–HP treatment leads to an increase in the size of the dislocation loops, as seen by comparing the TEM images of the samples T1-3, T2 and T3. Note that the small stressed areas do not appear in the samples T1-2, T1-3 and T2 but are present in the sample T3.

The surface image of the sample T1-2 after selective etching exhibits the presence of hillocks in concentration of 2.5×10^6 cm^{-2}. This value is practically the same as that of the sample T1-1, treated at low pressure. The average hillock size for the sample T1-2 is higher than that for the sample T1-1. Selective etching on the samples T1-3, T2 and T3 shows the appearance of small defect clusters additionally to the OPs (Fig. 4). As can be seen from the surface images of these samples, the increase in the temperature of the HT–HP treatment is followed by an increase in the size of the defect clusters. We have to emphasize that the size of these defects observed by microscopy after selective etching is not the real one. In fact, the measured defect size depends on the stress near the defect and on the etching time. The defect size measured by the selective etching technique is an effective parameter typically larger than the actual size of the defect. Consequently, the defect size and density can be used only for comparison between images of different samples. They cannot be compared with the TEM data. These small clusters, when in high concentration, mask the images of the OPs revealed by the selective etching. However, we know that the OPs are present from the TEM results. This indicates that the OPs introduced due to the HT-HP treatment were not destroyed during neutron irradiation and subsequent annealing. Additionally, we present in Fig. 5 the typical surface image after selective etching of another sample, not subjected to neutron irradiation, but HT–HP treated at $T = 1100$ °C, $P = 10$ kbar, $t = 5$ h. One can see hillocks, which most likely correspond to OPs surrounded by dislocation loops, but not the small defect clusters seen in the images of the samples T1-3, T2 and T3.

Similar results to that observed by TEM are also obtained from x-ray reciprocal space maps for the samples T1-3, T2 and T3. The defect dimensions estimated from rocking curves are presented in Table 2. The normal value of the rocking curve Full Width at Half Maximum (FWHM) for silicon crystals in this configuration of measurements is 15 arcsec. The values of the FWHM determined from rocking curves are higher than the normal and practically the same for all samples. This increase of the (FWHM) can be

Table 2 Defect dimensions and Full Width at Half Maximum (FWHM) values estimated from X-ray reciprocal space maps and rocking curves.

sample	defect dimension (nm)	FWHM (arcsec)
T0	41.5	19
T1-1	30	19
T1-2	40	19
T1-3	35	20
T2	46.5	20
T3	–	19

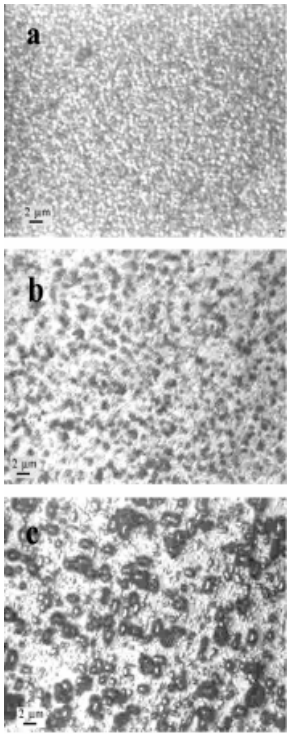

Fig. 4 Surface images after selective etching for samples (a) T1-3, (b) T2 and (c) T3.

connected with the presence of radiation-induced defects, having practically the same high concentration. One can see that the defect dimensions increase in the sample T2 as compared to the sample T1-3 (Table 2), in agreement with the TEM images. It is worth noting that the defect dimensions cannot be calculated accurately in the case of the sample T3 due to the additional presence of the small defects, which affect the view of the reciprocal space maps. For this sample, the small defects revealed by selective etching become large, so that their presence could not be registered by the applied X-ray diffraction method.

4 Discussion

The OPs surrounded by dislocation loops are the typical defects observed by TEM in HT as well as in HT–HP treated silicon [3, 14]. For treatments at atmospheric pressure [15, 16] these dislocation loops form adjacent to the precipitates if the temperature of the treatment is higher than 850 °C. They also form 1 in case of thermal treatments under enhanced pressure. Surface images after selective etching of silicon samples treated at a temperature higher than 600 °C typically show [13] the appearance of the OP-related hillocks. Enhanced hydrostatic pressure applied during heat treatment leads [13] to a decrease in the hillocks' size and an increase in their concentration. The high pressure favours the creation of small size defect agglomerates against the creation of large size agglomerates.

In a non-ideal crystal with grown-in defects, HP is generally expected [1] to generate new defects. Note, that selective etching measurements do not reveal the presence of additional types of defects, in HT–HP treated Si samples, if the temperature of the treatment is the same or higher than 900 °C [3, 7]. In our samples, we have additionally introduced radiation defects created after neutron bombardment and subsequent annealing at 400 °C. Both optical images of surface after selective etching and TEM images confirm the presence of some relatively small defects (compare for instance Fig. 4 and Fig. 5), due to their decoration with radiation-induced defects. Based on the fact that HP-related centers tend [13] to increase in size and decrease in concentration when the temperature of the HT–HP treatment increases, we suggest that the detected small defects in our samples are most likely HP-related centers. We stress that this behavior is the opposite of that observed in only HT–HP treated samples (Fig. 5), as we mentioned in the previous paragraph.

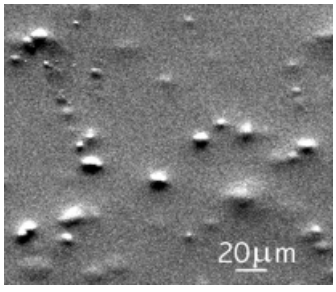

Fig. 5 Surface images after selective etching for sample treated at 1100 °C, 10 kbar, 5 h.

It is generally known that vacancy-type defects [2, 15, 17, 18] interact with oxygen and affect the nucleation process of the TDs and OPs. Additionally, the spatial distribution of the TDs in the high energy ion implanted silicon, treated at HT–HP conditions, allows one to state that the vacancy-type nucleation sites are introduced in higher concentration, resulting in an increase of the donor formation rate [6]. In our case of neutron-irradiated HT–HP treated silicon, we have to take into account the presence of some silicon interstitial complexes as well. Our suggestion has as follows. Due to the initial HT–HP treatment small vacancy-type defects were introduced in the crystal. Additionally, the neutron irradiation introduces vacancies and interstitials of equal concentration. However, it is known that the vacancies, besides annihilation with self interstitials ($V + Si_I \rightarrow \varnothing$), form some vacancy-type complexes and also interact with grown-in defects and impurities. Therefore, some of the silicon interstitials remain in the crystal forming complexes. Note that at room temperature the single silicon interstitials are not stable, but the di-interstitials are [19]. Thus, the surplus silicon interstitials introduced in the course of neutron irradiation may either annihilate with the HT–HP induced vacancy-type defects or decorate them, if there is a barrier for the annihilation process [20]. The annihilation process of the additional HP-related defects with radiation-induced defects is not as effective as it is between radiation defects themselves, due to the relaxation in the silicon crystalline lattice during HP heat treatment. Actually, the formation of the vacancy-type defects during the HP treatment is followed by displacements of the neighbouring host atoms from their regular sites, in order for the free volume to be created around the vacancy-type defects. In order for the annihilation process to take place these neighbouring atoms should first return to their initial sites and then annihilate with the vacancy-type defects. This means that the barrier for the annihilation process is increased. If this barrier cannot be surpassed, decoration of the vacancy-type defects is likely to occur. Thus, it is reasonable to conclude that the small defect clusters detected in the present study are most likely the HP-related vacancy-type defects decorated with neutron irradiation-induced defects.

Theoretical investigations dealing with the pressure dependence of the vacancy mechanism in Si have concluded [21, 22] that the effect of pressure on the formation of vacancies is very weak and therefore the concentration of vacancies is not really affected. At first sight, this seems to be in contrast with our results. However, it is possible that the application of high pressure does not directly influences the production of vacancies by the vacancy mechanism, but influences the production of vacancies by another process. For instance, it is known that the application of pressure affects the oxygen precipitation process. The formation of oxygen precipitates is followed by an inflow of vacancies towards the precipitate area in order to create the extra free volume needed and an outflow of silicon interstitials at the Si/SiO_x boundary. So finally, there is an increase in the vacancy concentration in the matrix, indirectly caused by the application of external pressure.

Enhanced formation of the “old” and “new” thermal donors was observed [6] in high-energy implanted silicon annealed in the temperature range of 450–1050 °C. This effect occurs only in irradiated layers where the vacancy-type defects dominate. It has therefore been concluded [6] that the vacancy-type defects most likely serve as nuclei for TDs. The present results indicate the appearance of additional vacancy-type defects after HP treatment. Thus, going a step further, and considering that the samples have been subjected to a thermal anneal, which can produce TDs, we may assume that the small defect clusters observed could also serve as nucleation sites for the formation process of TDs.

5 Conclusion

Defects formed in Czochralski grown silicon heat-treated at 900–1050 °C under high hydrostatic pressures up to 12 kbars are investigated. Their decoration with radiation defects introduced by neutron irradiation and subsequent anneals, allows their detection. They are small defects, most likely vacancy-type, which form under HT–HP conditions, besides the oxygen precipitates and the dislocation loops. We suggest that they are HP-related centers, as they tend to increase in size and decrease in concentration when the temperature of the HT–HP treatment increases. They serve as nucleation sites for clusters of radiation defects.

Acknowledgements This work was supported in part by Polish Committee for Scientific Research (grant no. 9T11B 072 19) and by INTAS (grant # INTAS-01-0468). The help of Mr. M. Prujszczyk from IET Warsaw in sample treatment is gratefully acknowledged.

References

[1] J. Jung and M. Lefeld-Sosnowska, Phil. Mag. **50**, 233 (1984).
[2] H. Bender and J. Vanhellemont, in: Handbook in Semiconductors, edited by S. Mahayan, (Elsevier Science B.V., North-Holland, **3b**, 1994), p. 1637.
[3] A. Romano-Rodriguez, A. Bachrouri, M. Lopez, J. R. Morante, A. Misiuk, B. Surma, and J. Jun, Mater. Sci. Eng. **B73**, 250 (2000);
A. Misiuk, B. Surma, and J. Hartwig, Mater. Sci. Eng B **36**, 30 (1996);
A. Misiuk, W. Jung, B. Surma, J. Jun, and M. Rozental, Solid State Phenom. **57–58**, 383 (1997).
[4] E. P. Neustroev, I. V. Antonova, V. F. Stas, V. P. Popov, and V. I. Obodnikov, Physica B **270**, 1 (1999);
E. P. Neustroev, I. V. Antonova, V. P. Popov, D. V. Kilanov, and A. Misiuk, Physica B **293**, 44 (2000).
[5] V. V. Emtsev, B. A. Andreev, A. Misiuk, W. Jung, and K. Scmalz, Appl. Phys. Lett. **71**, 264 (1997);
A. Misiuk, phys. stat. sol. (a) **171**, 191 (1999).
[6] E. P. Neustroev, I. V. Antonova, V. P. Popov, V. F. Stas, V. A. Skuratov, and A. Yu. Dyduk, Nucl. Instrum. Methods B **171**, 443 (2000);
I. V. Antonova, E. P. Neustroev, A. Misiuk, and V. A. Skuratov, Solid State Phenom. **82–84**, 243 (2002).
[7] I. V. Antonova, A. Misiuk, V. P. Popov, L. I. Fedina, and S. S. Shaimeev, Physica B **225**, 251 (1996).
[8] H. Stein, in 2nd Intern. Conf. Neutron Transmutation Doping in Semiconductors, edited by J. Meese, (Plenum Press, New York, 1979), p. 229.
[9] Y. H. Lee, J. C. Corelli, and J. W. Corbett, Phys. Lett. **60A**, 55 (1977).
[10] J. L. Linström and B. G. Svensson, Mater Res. Symp. Soc. Proc. **Vol. 59**, 45 (1986).
[11] C. A. Londos, I. V. Antonova, M. Potsidou, A. Misiuk, J. Bak-Misiuk, and A. K. Gutakovskii, J. Appl. Phys. **91**, 1198 (2002).
[12] S. J. Pearton, J. W. Corbett, and M. Stavola, Hydrogen in Crystalline Semiconductors, (Springer-Verlag, Berlin, 1992) Chap. 8.
[13] I. V. Antonova, A. Misiuk, V. P. Popov, A. E. Plotnikov, and B. Surma, Physica B **253**, 131 (1998).
[14] H. Bender, phys. stat. sol. (a) **86**, 245 (1984).
[15] A. Borghesi, B. Pivac, A. Sassella, and A. Stella, J. Appl. Phys. **77**, 4169 (1995).
[16] H. Fujimori, J. Electrochem. Soc. **144**, 3180 (1997).
[17] S. M. Hu, J. Appl. Phys. **52**, 3974 (1981).
[18] R. S. Brusa, W. Deng, G. P. Karwasz, A. Zecca, and D. Pliszka, Appl. Phys. Let. **79**, 1492 (2001).
[19] J. W. Corbett, J. P. Kavins, and T. Y Tan, Nucl. Instrum. Methods Phys. Res. B **182–183**, 457 (1981).
[20] L. I. Fedina, A. K. Gutakovskii, L. A. Aseev, J. Van Landuyt, J. Vanhellemont, phys. stat. sol. (a) **171**, 147 (1999).
[21] A. Antonelli and J. Bernholc, Phys. Rev. B **40**, 10643 (1989).
[22] A. Antonelli, E. Kaxiras, and D. J. Chadi, Phys. Rev. Lett. **81**, 2088 (1998).